ACS APPLIED MATERIALS & INTERFACES

Research Article

www.acsami.org

9-Arylidene-9*H*-Fluorene-Containing Polymers for High Efficiency Polymer Solar Cells

Qian Liu,[†] Cuihong Li,*[,†] Enquan Jin,[†] Zhen Lu,[†] Youchun Chen,[‡] Fenghong Li,[‡] and Zhishan Bo*[,†]

[†]Beijing Key Laboratory of Energy Conversion and Storage Materials, College of Chemistry, Key Laboratory of Theoretical and Computational Photochemistry, Ministry of Education, Beijing Normal University, Beijing 100875, China

[‡]State Key Laboratory of Supramolecular Structure and Materials, Jilin University, Changchun 130012, People's Republic of China

Supporting Information

ABSTRACT: 9-Arylidene-9*H*-fluorene containing donor−acceptor (D−A) alternating polymers **P1** and **P2** were synthsized and used for the fabrication of polymer solar cells (PSCs). High and low molecular weight **P1** (**HMW-P1** and **LMW-P1**) and high molecular weight **P2** were prepared to study the influence of molecular weight and the position of alkoxy chains on the photovoltaic performance of PSCs. **HMW-P1**:$PC_{71}BM$-based PSCs fabricated from 1,2-dichlorobenzene (DCB) solutions showed a power conversion efficiency (PCE) of 6.26%, while **LMW-P1**:$PC_{71}BM$-based PSCs showed poor photovoltaic performance with a PCE of only 2.75%. PCE of **HMW-P1**:$PC_{71}BM$-based PSCs was further increased to 6.52% with the addition of 1,8-diiodooctane (DIO) as the additive. Meanwhile, PCE of only 2.51% was obtained for **P2**:$PC_{71}BM$-based PSCs. The results indicated that the position of alkoxy substituents on the 9-arylidene-9H-fluorene unit and the molecular weight of polymers are very crucial to the photovoltaic performance of PSCs.

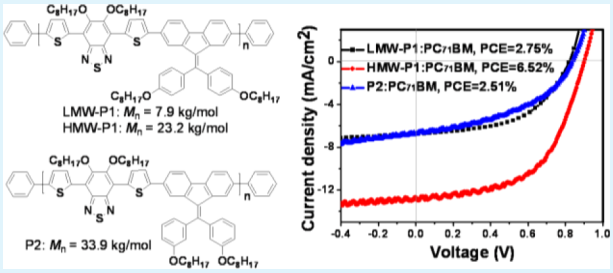

KEYWORDS: *conjugated polymers, bulk heterojunction, polymer solar cells, Suzuki polycondensation, benzothiadiazole, donor−acceptor alternating polymers*

INTRODUCTION

Great efforts have been devoted to the studies of polymer solar cells (PSCs) in the past two decades,[1−12] and recently efficiency higher than 9% has been achieved by several groups.[13−17] The donor−acceptor (D−A) blending active layer of PSCs is in a bulk heterojunction (BHJ) structure with a thickness of about 100 nm. The excitons can effectively dissociate at the D−A interfaces to form free charges, which can be further transported to the collecting electrodes via the interpenetrating D−A networks.[18−29] The HOMO and LUMO energy levels can be adjusted by using different donor or acceptor in the main chain of polymer via the intramolecular charge transfer (ICT). Many D−A alternating polymers have been synthesized and used as donor materials for PSCs.[1−29] 9,9-Dialkylfluorene and benzothiadiazole based D−A alternating conjugated polymers are of deep HOMO levels, and the formed PSCs are usually of high open circuit voltage.[30] The first polyfluorene containing D−A alternating copolymer (PFDTBT) used as donor material in BHJ PSCs was reported in 2003 and a PCE of 2.2% was achieved.[31] The low PCE is the result of the low photocurrent and fill factor (FF). The changing of lateral substituents of PFDTBT has been investigated by several groups, and the PCE has been enhanced to 4.5%.[32] The two bulky side chains at the 9-position sp^3-hybridized carbon of fluorene can hinder the close packing of polymer chains in film and result in lower hole mobility.[32] To make polymers that can closely pack in solid state, we and Dai et al. have reported 9-alkylidene-9H-fluorene based copolymers PAFDTBT.[33,34] Different from 9,9-dialkyl-substituted fluorene, the 9-alkylidene-9H-fluorene tend to keep a planar conformation, which can enhance the $\pi-\pi$ stacking of polymer chains in film and thus can increase the hole mobility. A PCE of 4.8% has been achieved for PAFDTBT:$PC_{71}BM$-based PSCs fabricated from 1,2-dichlorobenzene (DCB) solutions. PCE can be further improved to 6.2% by using 0.5 vol % DIO as the additive. Here we reported the synthesis of two kinds of 9-arylidene-9H-fluorene-containing D−A alternating copolymers (**P1** and **P2** as shown in Chart 1) used for high efficiency polymer solar cells. The introduction of two aryl substituents can extend the lateral conjugation of polymer chains, which maybe help to facilitate the interchain charge transport. Low and high molecular weight polymers (**LMW-P1** and **HMW-P1**) and high molecular weight **P2** have been synthesized and tested for PSCs. We have found that the molecular weight and the position of alkoxy substituents on the 9-arylidene-9H-fluorene unit are very crucial to the photovoltaic performance of PSCs. It is worthy noting that the huge influence of side chains on the performance of PSCs has also been reported recently by Zhuang and Andersson et al.[35] **LMW-P1**:$PC_{71}BM$-based PSCs showed poor photovoltaic performance with a PCE of only

Received: October 9, 2013
Accepted: January 15, 2014
Published: January 15, 2014

dx.doi.org/10.1021/am404437y | *ACS Appl. Mater. Interfaces* 2014, 6, 1601−1607

Chart 1. Chemical Structures of Polymer P1 and P2

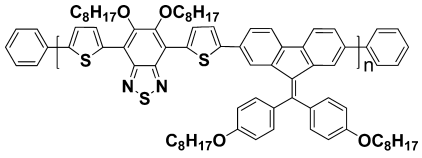

P1

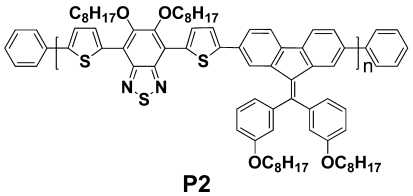

P2

2.75%; whereas **HMW-P1**:$PC_{71}BM$-based PSCs fabricated from DCB solutions showed a PCE of 6.26%. When 0.125 vol % 1,8-diiodooctane (DIO) was used as the additive, PCE of **HMW-P1**:$PC_{71}BM$-based PSCs was further increased to 6.52%. High PCE without using any additive in fabrication of PSCs makes **HMW-P1** a promising donor material for practical applications. We also found that the position of the flexible side chains is also very crucial to the PCE of devices. Although high molecular weight **P2** was used for the fabrication of PSCs, a PCE of only 2.51% was achieved. TEM studies revealed that the **HMW-P1**:$PC_{71}BM$ blend films are composed of homogeneous nanostructures without apparent phase separation; while for the **P2**:$PC_{71}BM$ blend films, isolated $PC_{71}BM$ nano islands are formed with apparent phase separation.

RESULTS AND DISCUSSION

Material Synthesis and Characterization. The syntheses of monomers **M1** and **M2** and polymers **P1** and **P2** are outlined in Scheme 1. Starting from commercially available bis(4-hydroxyphenyl)methanone, its reaction with *n*-octylbromide under K_2CO_3/acetone conditions afforded bis(4-(octyloxy)phenyl)methanone (**1**) in a yield of 96%. The treatment of **1** and 2,7-dibromofluorenone with Lawesson's reagent in refluxed toluene afforded the cross coupling product **2** in a yield of 39%.[36] The reaction of 2 with bis(pinacolato)-diboron under Miyaura reaction conditions furnished **M1** in a yield of 71%. The synthesis of **M2** is started from 1-bromo-3-(octyloxy)benzene, its treatment with *n*-BuLi at −78 °C was followed by quenching the resulted anions with 3-(octyloxy)-benzaldehyde to give bis(3-(octyloxy)phenyl)methanol (**3**) in a yield of 65%. The oxidation of **3** with pyridinium chlorochromate in DCM afforded bis(3-(octyloxy)phenyl)-methanone (**4**) in an 80% yield. Cross coupling of **4** and 2,7-dibromofluorenone with Lawesson's reagent afforded **5** in a yield of 34%, which was converted to **M2** in a yield of 36% by reaction with bis(pinacolato)diboron. Suzuki-Miyaura polycondensation of bis(boronic acid pinacol ester) monomers **M1** and **M2** with dibromo monomer **M3** in a biphasic mixture of toluene and aqueous $NaHCO_3$ using freshly prepared Pd-$(PPh_3)_4$ as the catalyst precursor and tetrabutylammonium bromide (TBAB) as the phase transfer catalyst (PTC) afforded **P1** and **P2** in yields of 78% and 75%, respectively. The chemical structures of **M1**, **M2**, **P1**, and **P2** were verified by ^1H and ^{13}C NMR spectroscopy and elemental analysis. To verify the influence of molecular weight on the photovoltaic performance of polymer solar cells, two polymer samples of **P1** with different molecular weight were prepared. The weight average molecular

Scheme 1. Synthesis of Monomers and Copolymers

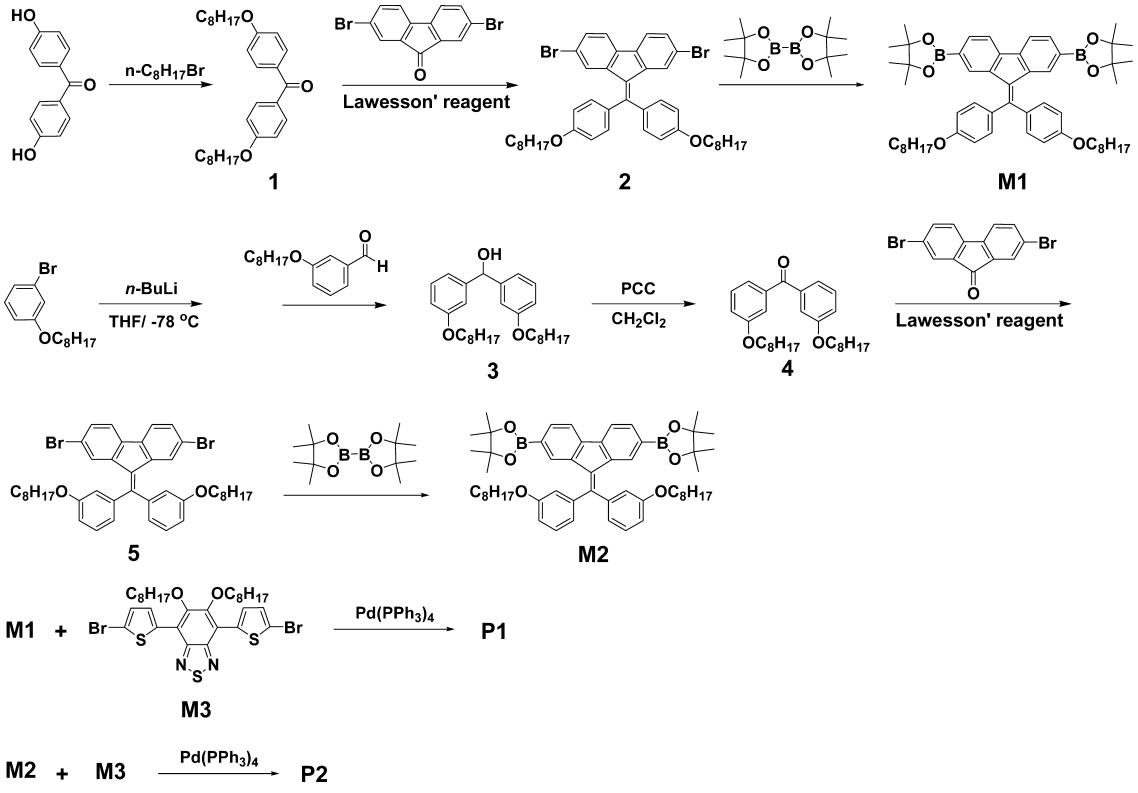

weights (M_w) for high molecular weight **P1** (**HMW-P1**), low molecular weight **P1** (**LMW-P1**), and **P2** are 53.4, 12.7, and 88.2 kg/mol with polydispersity indexes (PDIs) of 2.3, 1.6, and 2.6, respectively. **P1** and **P2** exhibited good thermal stability. As observed by thermogravimetric analysis (TGA), **P1** and **P2** showed 5% weight loss up to 325 and 315 °C, respectively, under a nitrogen atmosphere and the data are summarized in Table 1. There is no obvious glass transition for **P1** and **P2** in the differential scanning calorimetry (DSC) curves in the range of 50−260 °C at a heating rate of 20 °C/min.

Table 1. Molecular Weights and Thermal Properties of the Copolymers

polymer	M_n (kg/mol)	M_w (kg/mol)	PDI	T_d (°C)[c]
LMW-P1[a]	7.9	12.7	1.6	329
HMW-P1[b]	23.2	53.4	2.3	325
P2[b]	33.9	88.2	2.6	315

[a]M_n, M_w, and PDI were determined by GPC against polystyrene (PS) standards at room temperature with THF as an eluent. [b]determined by GPC at 150 °C with 1,2,4-trichlorobenzene as an eluent against PS standards. [c]Temperature at 5% weight loss.

Optical Properties. The optical properties of **P1** (**HMW-P1** and **LMW-P1**) and **P2** in DCB solutions (0.02 mg/mL) and as thin films (20 mg/mL in DCB) were investigated by UV-visible absorption spectroscopy and the spectra of **HMW-P1** and **P2** are shown in Figure 1. The absorption coefficients

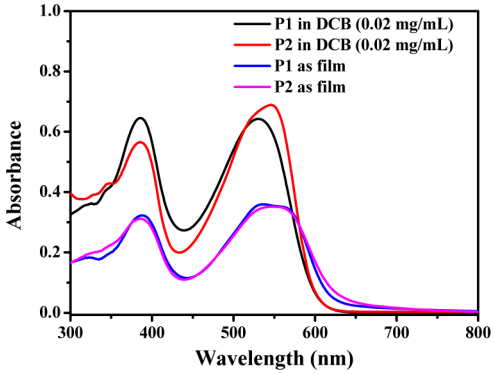

Figure 1. UV−vis absorption spectra of **P1** and **P2** in DCB solutions (0.02 mg/mL) and as films spin coated on quatz plates from DCB soltions (20 mg/mL).

of **LMW-P1**, **HMW-P1**, and **P2** in dilute DCB solutions (0.02 mg/mL) are 6.8×10^{-4}, 7.8×10^{-4}, and 8.0×10^{-4} L/mol·cm, respectively. It is worthy noting that **HMW-P1** and **LMW-P1** displayed almost exactly the same absorption spectra both in solutions and as thin films, therefore we use **P1** without differentiating **HMW-P1** and **LMW-P1.** In DCB solution, **P1** exhibited two broad absorption bands ranging from 300 to 440 nm and from 440 to 640 nm with two maxima located at 387 and 530 nm, respectively. **P2** in DCB solution displayed similar absorption spectrum with two absorption maxima peaked at 385 and 544 nm, respectively. The high energy bands are attributed to the $\pi-\pi^*$ transition; whereas the low energy bands are due to the ICT between the donor and acceptor units. On going from solutions to films, the absorption spectra of both **P1** and **P2** became broad and red-shifted. As thin films, **P1** displayed two peaks located at 388 and 537 nm and **P2** showed two peaks located at 386 and 550 nm. The broadening and red-shifting of film absorption spectra are due to the aggregation of polymer chains in solid state. The film absorption onsets of **P1** and **P2** are 620 and 630 nm, corresponding to optical band gaps of 2.0 and 1.97 eV, respectively. The data are summarized in Table 2.

Table 2. Physical, Electronic, and Optical Properties of P1, P2, and P3.

polymer	λ_{max} (nm) solution	λ_{max} (nm) film	$E_{g,opt}$ (eV)[a]	HOMO (eV)	LUMO (eV)[b]
P1	387, 530	388, 537	2.0	−5.41	−3.41
P2	385, 544	386, 550	1.97	−5.44	−3.47

[a]Calculated from the absorption band edge of the copolymer film, $E_{g,opt} = 1240/\lambda_{edge}$. [b]Calculated by the equation $E_{LUMO} = E_{HOMO} + E_{g,opt}$.

Electrochemical Properties. The electrochemical properties of **P1** and **P2** were investigated by cyclic voltammetry using 0.1 M NBu_4BF_4 acetonitrile solution as the supporting electrolyte.[37] As shown in Supporting Information Figure S1, in the scanning range of 0 to 1.5 V **P1** and **P2** showed reversible cyclic voltammetry diagrams. The onset oxidation potentials of **P1** and **P2** are 0.70 and 0.73 V, respectively. According to the following equation $E_{HOMO} = -e(4.71 + \Phi_{ox}(Ag/Ag+))$ (eV), the HOMO energy levels (E_{HOMO}) of **P1** and **P2** were determined to be −5.41 and −5.44 eV, respectively. And the LUMO energy levels (E_{LUMO}) of **P1** and **P2** were calculated to be −3.41 and −3.47 eV, respectively, according to the equation $E_{LUMO} = E_{HOMO} + E_{g,opt}$. The data are summarized in Table 2. The LUMO energy levels of **P1** and **P2** are positioned about 0.80 eV above that of $PC_{71}BM$ (−4.2 eV), which offer enough driving force for charge separation and transfer without too much energy loss.[38−44] When blended with $PC_{71}BM$ acceptor, their low-lying HOMO energy level will afford a high V_{oc} in PSCs.

Photovoltaic Properties. Photovoltaic devices were fabricated using a conventional device structure ITO/PEDOT:PSS/active layer/LiF/Al and measured under the illumination of AM 1.5G (100 mW/cm^2).[45−51] The active layer is a blend of polymer and $PC_{71}BM$ and the film thickness is controlled at about 100 nm. Three polymer samples (**HMW-P1**, **LMW-P1**, and **P2**) were tested as donor materials for the fabrication of PSCs. A series of studies were carried out to improve the PCE of photovoltaic cells. The weight ratio of donor to acceptor, the thickness of active layer, the processing solvent, and the additive were screened to optimize the device fabrication conditions. The current density−voltage ($J-V$) characteristics are shown in Figure 2. After optimization, PSCs based on **LMW-P1**:$PC_{71}BM$ (1:2, by weight) fabricated from pure DCB solutions (30 mg/mL) in a spin-coating speed of 1500 rpm showed a PCE of 1.95% with a V_{oc} of 0.86 V, a short circuit current (J_{sc}) of 5.10 mA cm^{-2}, and a fill factor (FF) of 0.44. When 0.5% DIO was used as an additive, the PCE of **LMW-P1** based PSCs could be improved to 2.75%. When high molecular weight **HMW-P1** was used instead of low molecular weight **LMW-P1**, the photovoltaic performances were markedly enhanced. **HMW-P1** to $PC_{71}BM$ is 1:3 by weight, the blend concentration is 28 mg/mL in DCB, and the spin-coating speed is 1800 rpm. PCE of 6.26% with a V_{oc} of 0.94 V, a J_{sc} of 11.28 mA cm^{-2}, and an *FF* of 0.59 was obtained for PSCs fabricated. The use of 0.125% DIO as the additive, the PCE was only slightly increased to 6.52% with a V_{oc} of 0.90 V, a J_{sc} of 12.72

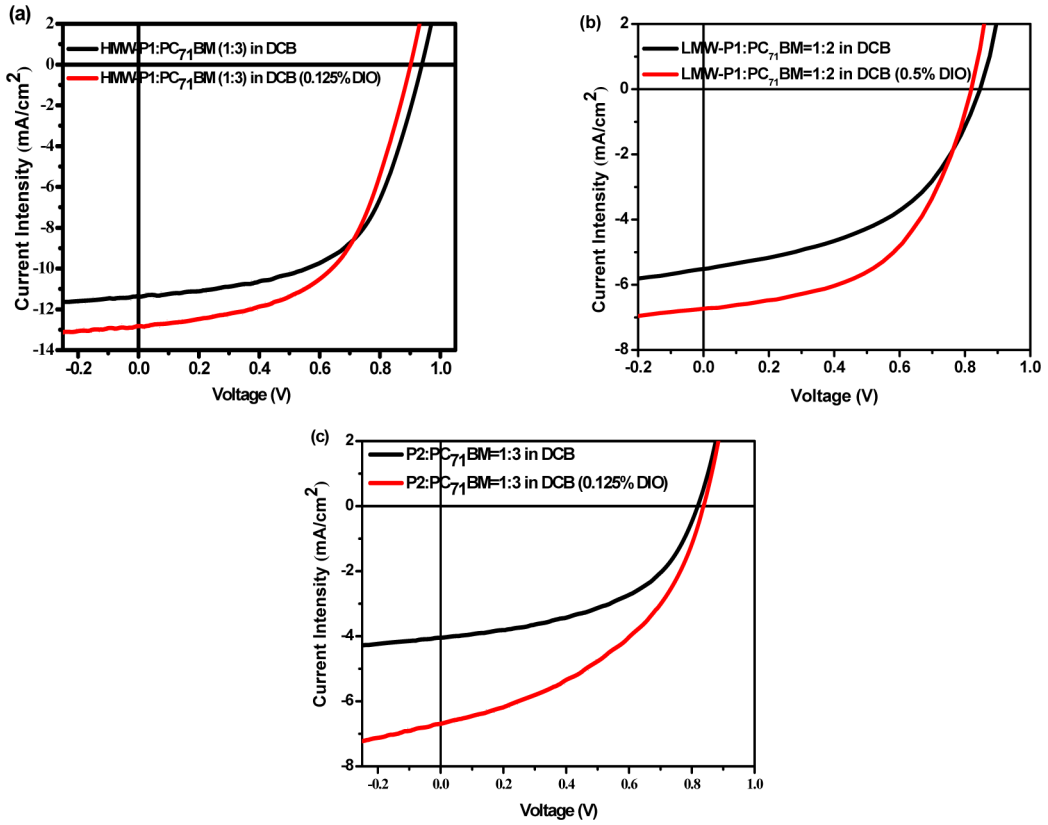

Figure 2. *J*–*V* curves for the BHJ solar cells derived from the blend of **HMW-P1**:$PC_{71}BM$ (a), **LMW-P1**:$PC_{71}BM$ (b), and **P2**:$PC_{71}BM$ (c) in DCB with (red line) and without (black line) DIO.

mA cm^{-2}, and an FF of 0.57. It is worthy noting that for high molecular weight polymer **HMW-P1**, the PCE is not very sensitive to the additive. Although the influence of molecular weight on the photovoltaic performance of devices was reported by several groups before,[47,52−54] such a dramatic PCE difference caused by molecular weight difference is unusual. To investigate the influence of the position of alkoxy substituents on the photovoltaic performance, **P2** with the octyloxy substituent on the meta position of phenyl ring was also synthesized and tested as donor material. Although high molecular weight **P2** was used for the fabrication of PSCs, the achieved highest PCE was only 2.51% at the same fabrication conditions as **HMW-P1**. The use of 0.125% DIO as the additive led to a decrease of PCE to 1.67%. The detailed conditions for the fabrication of PSCs and the photovoltaic parameters are summarized in Table 3. To corroborate the J_{sc} measurement results, external quantum efficiencies (EQEs) of solar cells were measured under the monochromatic light illumination. As shown in Figure 4, a significant photo-to-current response can be seen from 370 to 570 nm with EQE values of 55-68% for the optimized devices based on **HMW-P1**:$PC_{71}BM$ (1:3) fabricated from DCB solutions without and with DIO. The EQE curves of **P2**:$PC_{71}BM$ (1:3) based devices fabricated from DCB solutions without and with DIO are also shown in Figure 3. **P2**:$PC_{71}BM$ (1:3) based solar cells exhibited markedly weaker EQE response with the maximum value of about 45%. The J_{sc} calculated from integration of the EQE with an AM 1.5G reference spectrum agreed roughly with the J_{sc} obtained from the *J*–*V* measurements for both **HMW-P1** and **P2**. The obvious difference in EQE leads to the big difference in J_{sc} of the two polymers with the very similar structure. This high EQE response and high J_{sc} of **HMW-P1** lead to high PCE. For **P2** which has the low PCE, the EQE and J_{sc} are lower than **HMW-P1**.

Table 3. Photovoltaic Parameters of LMW-P1:$PC_{71}BM$, HMW-P1:$PC_{71}BM$, and P2:$PC_{71}BM$ Fabricated from DCB with or without DIO

active layer	solvent	V_{oc} (V)	J_{sc} (mA/cm^2)	FF	PCE (%)	thickness (nm)
LMW-P1:$PC_{71}BM$ (1:2)	DCB	0.86	5.10	0.44	1.95	100
	DCB[a]	0.89	5.03	0.62	2.75	102
HMW-P1:$PC_{71}BM$ (1:3)	DCB	0.94	11.28	0.59	6.26	100
	DCB[b]	0.90	12.72	0.57	6.52	104
P2:$PC_{71}BM$ (1:3)	DCB	0.83	6.88	0.44	2.51	102
	DCB[b]	0.82	4.00	0.51	1.67	100

[a]Containing DIO (0.5%, by volume). [b]Containing DIO (0.125%, by volume).

Transport Properties. The transport properties of **LMW-P1**, **HMW-P1**, and **P2** were investigated by fabricating bottom-gate, top-contact organic thin film field effect transistors (FETs).[47] The pristine **LMW-P1** films showed a hole mobility of 4.2×10^{-5} cm^2 V^{-1} s^{-1} with an on/off current ratio of 10^2; whereas the pristine **HMW-P1** films exhibited a hole mobility of 2.3×10^{-4} cm^2 V^{-1} s^{-1} with an on/off current ratios of 10^3. The results clearly indicated that the molecular weight of polymers also played a very important role in their transport behaviors. To understand why molecular weight has such a distinct influence on the hole mobility of polymers, the packing of polymer chains in solid state was investigated by using X-ray diffraction (XRD) technique. XRD patterns of **HMW-P1** and

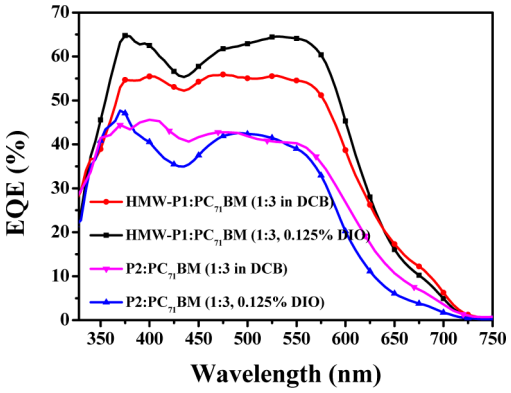

Figure 3. EQE curves of the solar cells based on the **HMW-P1**:$PC_{71}BM$ (1:3, w/w) and **P2**:$PC_{71}BM$ (1:3, w/w) blend in DCB with and without 0.125 vol % DIO.

LMW-P1 are shown in Figure S2 in the Supporting Information. XRD patterns of **HMW-P1** and **LMW-P1** are slightly different. XRD pattern of **HMW-P1** displayed two intense peaks at 2θ = 4.32° and 20.38°; whereas **LMW-P1** showed three less intensive diffraction peaks at 2θ = 4.48°, 11.87°, and 20.09°. The first diffraction peak at 2θ = 4.32° for **HMW-P1** and 2θ = 4.48° for **LMW-P1** reflexes the ordered packing of polymer chains separated by alkyl chains, corresponding to the *d* space of 20.45 Å for **HMW-P1** and 19.70 Å for **LMW-P1**. The diffraction peak at 2θ = 20.38° for **HMW-P1** and 2θ = 20.09° for **LMW-P1** reflexes the $\pi-\pi$ stacking distance between the polymer chains, which are 4.36 Å for **HMW-P1** and 4.42 Å for **LMW-P1**. From the above result, we can find that the packing of polymer chains in the solid state is also slightly influenced by the molecular weight of polymers. The hole mobility of the pristine **P2** films is 4.8×10^{-4} cm^2 V^{-1} s^{-1} with an on/off current ratio of 10^3. The output and transfer characteristic curves of the related polymer film FETs are shown in Supporting Information Figure S3.

Film Morphologies. Since the morphology of blend films can largely affect charge separation and transport, the surface morphology of the **LMW-P1**:$PC_{71}BM$ (1:2), **HMW-P1**:$PC_{71}BM$ (1:3), and **P2**:$PC_{71}BM$ (1:3) blend films spin-coated from DCB solutions without and with 0.5 vol % or 0.125 vol % DIO as the additive was investigated by atomic force microscopy (AFM) in tapping mode.[11] As shown in Supporting Information Figure S4, the blend films of both **LMW-P1**:$PC_{71}BM$ and **HMW-P1**:$PC_{71}BM$ prepared by spin-coating from DCB solutions showed similar surface morphology with quite small phase separation. The root-mean-square (rms) values of **LMW-P1**:$PC_{71}BM$ and **HMW-P1**:$PC_{71}BM$ blend films are 0.43 and 0.68 nm, respectively. The use of 0.5 vol % DIO as additive for the preparation of the blend films, the surface morphology of **LMW-P1**:$PC_{71}BM$ blend films did not exhibit a marked change and the rms value is almost unchanged. For the **HMW-P1**:$PC_{71}BM$ blend films, when 0.125 vol % DIO was used, the surface morphology became smoother and the rms value decreased to 0.40 nm. The **P2**:$PC_{71}BM$ (1:3) blend films spin-coated from DCB solutions without and with 0.125 vol % DIO showed quite smooth surface morphology with almost the same rms value (0.35 and 0.33 nm, respectively). To really understand the large difference of device performance for **HMW-P1** and **P2** based PSCs, transmission electron microscopy (TEM) experiments were conducted for the blend films and the images are shown in Figure 4. As shown in Figure 4a and 4b, TEM images of **HMW-P1**:$PC_{71}BM$ blends spin-coated from DCB solutions without and with 0.125% DIO as the processing additive are both homogenous without apparent phase separation. The high-magnification TEM images of **HMW-P1**:$PC_{71}BM$ blends (4e and 4f) indicated that nanoscale phase separation is formed. As shown in Figure 4c and 4d, TEM images of the **P2**:$PC_{71}BM$ blend films spin-coated from DCB solutions without and with 0.125% DIO as the processing additive exhbited similar nanostructures. Isolated nano islands, which are probably formed by the aggregation of $PC_{71}BM$, are embedded in the homogenous blend films. As shown in Figure 4g and 4h, the high-magnification TEM images of **P2**:$PC_{71}BM$ blends clearly demonstrated that the isolated $PC_{71}BM$ nano islands are in a width of about 5 nm with a lenth in the range of 5−30 nm, indicating that the miscibility between **P2** and $PC_{71}BM$ is poorer than that between **P1** and $PC_{71}BM$. The TEM results

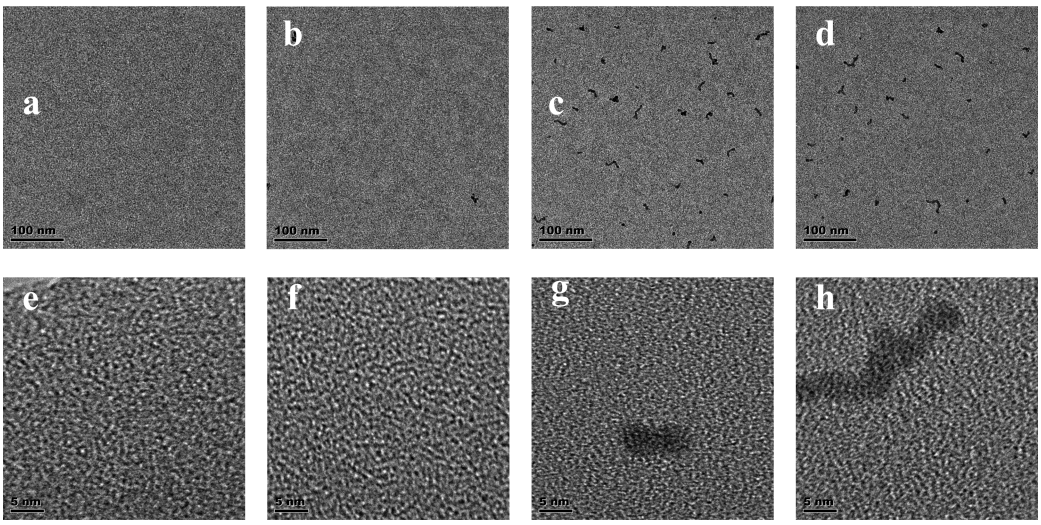

Figure 4. TEM images of **HMW-P1**:$PC_{71}BM$ blends (a), **HMW-P1**:$PC_{71}BM$ blends with 0.125% DIO (b), **P2**:$PC_{71}BM$ blends (c), and **P2**:$PC_{71}BM$ blends with 0.125% DIO (d); high-magnification TEM images of **HMW-P1**:$PC_{71}BM$ blends (e), **HMW-P1**:$PC_{71}BM$ blends with 0.125% DIO (f), **P2**:$PC_{71}BM$ blends (g), and **P2**:$PC_{71}BM$ blends with 0.125% DIO (h).

can clearly illustrate that the lower power conversion efficiency of **P2**:$PC_{71}BM$-based solar cells is caused by the poor film morphology of blend films. The isolated $PC_{71}BM$ nano islands are detrimental, since the formed electrons located on them can not be transported to the cathode very efficiently. The above results demonstrated that the position of alkoxy chains on the phenyl rings caused a great influence on the film morphology of blend films.

CONCLUSIONS

9-(Bis(4-(octyloxy)phenyl)methylene)-9*H*-fluorene or 9-(bis-(3-(octyloxy)phenyl)methylene)-9H-fluorene containing main chain D−A alternating copolymers **LMW-P1**, **HMW-P1**, and **P2** have been synthesized and used as donor materials for the fabrication of BHJ PSCs. The position of flexible side chains and the molecular weight of polymers played very important roles in determining the PCE of PSCs. PSCs with the **LMW-P1**:$PC_{71}BM$ (1:2) blend from DCB solutions as the active layer showed a PCE of only 1.95%; whereas the high molecular weight polymer **HMW-P1**:$PC_{71}BM$ (1:3)-based solar cells fabricated under the same conditions showed a PCE of 6.26%. The huge difference of PCE indicated that high molecular weight is crucial to achieve high efficiency. The PCE of **HMW-P1**:$PC_{71}BM$-based PSCs can be further improved to 6.52% by using 0.125 vol % DIO as the additive. The position of the flexible side chains is also crucial to the PCE of devices, although high molecular weight polymers were used for the fabrication of PSCs, the meta substituted polymer **P2** based PSCs only exhibited a PCE of 2.51%. TEM studies revealed that $PC_{71}BM$ showed better miscibility with **HMW-P1** than with **P2**. The **HMW-P1**:$PC_{71}BM$ blend films are of homogenous nanostructures; whereas **P2**:$PC_{71}BM$ blend films contain isolated $PC_{71}BM$ nano islands.

ASSOCIATED CONTENT

Supporting Information

Synthesis and characterizations of compounds and polymers, experimental details for the fabrication and characterization of organic field-effect transistors, experimental details for the fabrication and measurements of polymer solar cells, and ^{1}H NMR, ^{13}C NMR spectra. This material is available free of charge via Internet at http://pubs.acs.org.

AUTHOR INFORMATION

Corresponding Authors

*E-mail: licuihong@bnu.edu.cn.

*E-mail: zsbo@bnu.edu.cn.

Notes

The authors declare no competing financial interest.

ACKNOWLEDGMENTS

We express thanks for the financial support by the NSF of China (51003006, 91233205, and 21161160443), Beijing Natural Science Foundation (2132042), the 973 Programs (2011CB935702 and 2009CB623603), and the Fundamental Research Funds for the Central Universities.

REFERENCES

(1) Krebs, F. C. *Sol. Energy Mater. Sol. Cells* **2009**, *93*, 394−412.
(2) Kim, J. Y.; Lee, K.; Coates, N. E.; Moses, D.; Nguyen, T. Q.; Dante, M.; Heeger, A. J. *Science* **2007**, *317*, 222−225.
(3) Zhan, X. W.; Zhu, D. B. *Polym. Chem.* **2010**, *1*, 409−419.
(4) Small, C. E.; Chen, S.; Subbiah, J.; Amb, C. M.; Tsang, S. W.; Lai, T. H.; Reynolds, J. R.; So, F. *Nat. Photonics.* **2012**, *6*, 115−120.
(5) Li, W. W.; Roelofs, W. S. C.; Wienk, M. M.; Janssen, R. A. J. *J. Am. Chem. Soc.* **2012**, *134*, 13787−13795.
(6) Hou, J. H.; Chen, H. Y.; Zhang, S. Q.; Li, G.; Yang, Y. *J. Am. Chem. Soc.* **2008**, *130*, 16144−16145.
(7) Guo, X. G.; Zhou, N. J.; Lou, S. J.; Hennek, J. W.; Ortiz, R. P.; Butler, M. R.; Boudreault, P. L. T.; Strzalka, J.; Morin, P. O.; Leclerc, M.; Navarrete, J. T. L.; Ratner, M. A.; Chen, L. X.; Chang, R. P. H.; Facchetti, A.; Marks, T. J. *J. Am. Chem. Soc.* **2012**, *134*, 18427−18439.
(8) Gendron, D.; Leclerc, M. *Energy Environ. Sci.* **2011**, *4*, 1225−1237.
(9) Thompson, B. C.; Frechet, J. M. J. *Angew. Chem., Int. Ed.* **2008**, *47*, 58−77.
(10) Dennler, G.; Scharber, M. C.; Brabec, C. J. *Adv. Mater.* **2009**, *21*, 1323−1338.
(11) Brabec, C. J.; Gowrisanker, S.; Halls, J. J. M.; Laird, D.; Jia, S. J.; Williams, S. P. *Adv. Mater.* **2010**, *22*, 3839−3856.
(12) Chen, J. W.; Cao, Y. *Acc. Chem. Res.* **2009**, *42*, 1709−1718.
(13) He, Z. C.; Zhong, C. M.; Su, S. J.; Xu, M.; Wu, H. B.; Cao, Y. *Nat. Photonics* **2012**, *6*, 591−595.
(14) Li, W. W.; Furlan, A.; Hendriks, K. H.; Wienk, M. M.; Janssen, R. A. J. *J. Am. Chem. Soc.* **2013**, *135*, 5529−5532.
(15) You, J. B.; Dou, L. T.; Yoshimura, K.; Kato, T.; Ohya, K.; Moriarty, T.; Emery, K.; Chen, C. C.; Gao, J.; Li, G.; Yang, Y. *Nat. Commun.* **2013**, *4*, 1446.
(16) Dou, L. T.; Chang, W. H.; Gao, J.; Chen, C. C.; You, J. B.; Yang, Y. *Adv. Mater.* **2013**, *25*, 825−831.
(17) Dou, L. T.; Gao, J.; Richard, E.; You, J. B.; Chen, C. C.; Cha, K. C.; He, Y. J.; Li, G.; Yang, Y. *J. Am. Chem. Soc.* **2012**, *134*, 10071−10079.
(18) Yu, G.; Gao, J.; Hummelen, J. C.; Wudl, F.; Heeger, A. J. *Science* **1995**, *270*, 1789−1791.
(19) Yu, G.; Heeger, A. J. *J. Appl. Phys.* **1995**, *78*, 4510−4515.
(20) Albrecht, S.; Janietz, S.; Schindler, W.; Frisch, J.; Kurpiers, J.; Kniepert, J.; Inal, S.; Pingel, P.; Fostiropoulos, K.; Koch, N.; Neher, D. *J. Am. Chem. Soc.* **2012**, *134*, 14932−14944.
(21) Amb, C. M.; Chen, S.; Graham, K. R.; Subbiah, J.; Small, C. E.; So, F.; Reynolds, J. R. *J. Am. Chem. Soc.* **2011**, *133*, 10062−10065.
(22) Chen, H. C.; Chen, Y. H.; Liu, C. C.; Chien, Y. C.; Chou, S. W.; Chou, P. T. *Chem. Mater.* **2012**, *24*, 4766−4772.
(23) Chu, T. Y.; Lu, J. P.; Beaupre, S.; Zhang, Y. G.; Pouliot, J. R.; Wakim, S.; Zhou, J. Y.; Leclerc, M.; Li, Z.; Ding, J. F.; Tao, Y. *J. Am. Chem. Soc.* **2011**, *133*, 4250−4253.
(24) He, Z. C.; Zhong, C. M.; Huang, X.; Wong, W. Y.; Wu, H. B.; Chen, L. W.; Su, S. J.; Cao, Y. *Adv. Mater.* **2011**, *23*, 4636−4643.
(25) Liang, Y. Y.; Xu, Z.; Xia, J. B.; Tsai, S. T.; Wu, Y.; Li, G.; Ray, C.; Yu, L. P. *Adv. Mater.* **2010**, *22*, E135−E138.
(26) Price, S. C.; Stuart, A. C.; Yang, L. Q.; Zhou, H. X.; You, W. *J. Am. Chem. Soc.* **2011**, *133*, 4625−4631.
(27) Son, H. J.; Wang, W.; Xu, T.; Liang, Y. Y.; Wu, Y. E.; Li, G.; Yu, L. P. *J. Am. Chem. Soc.* **2011**, *133*, 1885−1894.
(28) Su, M. S.; Kuo, C. Y.; Yuan, M. C.; Jeng, U. S.; Su, C. J.; Wei, K. H. *Adv. Mater.* **2011**, *23*, 3315−3319.
(29) Zhou, H. X.; Yang, L. Q.; Stuart, A. C.; Price, S. C.; Liu, S. B.; You, W. *Angew. Chem., Int. Ed.* **2011**, *50*, 2995−2998.
(30) Inganas, O.; Zhang, F. L.; Andersson, M. R. *Acc. Chem. Res.* **2009**, *42*, 1731−1739.
(31) Svensson, M.; Zhang, F. L.; Veenstra, S. C.; Verhees, W. J. H.; Hummelen, J. C.; Kroon, J. M.; Inganas, O.; Andersson, M. R. *Adv. Mater.* **2003**, *15*, 988−991.
(32) Chen, M. H.; Hou, J.; Hong, Z.; Yang, G.; Sista, S.; Chen, L. M.; Yang, Y. *Adv. Mater.* **2009**, *21*, 4238−4242.
(33) Du, C.; Li, C. H.; Li, W. W.; Chen, X.; Bo, Z. S.; Veit, C.; Ma, Z. F.; Wuerfel, U.; Zhu, H. F.; Hu, W. P.; Zhang, F. L. *Macromolecules* **2011**, *44*, 7617−7624.
(34) Liu, J.; Choi, H.; Kim, J. Y.; Bailey, C.; Durstock, M.; Dai, L. M. *Adv. Mater.* **2012**, *24*, 538−542.

(35) Zhuang, W. L.; Bolognesi, M.; Seri, M.; Henriksson, P.; Gedefaw, D.; Kroon, R.; Jarvid, M.; Lundin, A.; Wang, E. G.; Muccini, M.; Andersson, M. R. *Macromolecules* **2013**, *46*, 8488−8499.
(36) Brunetti, F. G.; Gong, X.; Tong, M.; Heeger, A. J.; Wudl, F. *Angew. Chem., Int. Ed.* **2010**, *49*, 532−536.
(37) Pommerehne, J.; Vestweber, H.; Guss, W.; Mahrt, R. F.; Bassler, H.; Porsch, M.; Daub, J. *Adv. Mater.* **1995**, *7*, 551−554.
(38) Fang, G.; Liu, J.; Fu, Y. Y.; Meng, B.; Zhang, B. H.; Xie, Z. Y.; Wang, L. X. *Org. Electron.* **2012**, *13*, 2733−2740.
(39) Carle, J. E.; Andreasen, B.; Tromholt, T.; Madsen, M. V.; Norrman, K.; Jorgensen, M.; Krebs, F. C. *J. Mater. Chem.* **2012**, *22*, 24417−24423.
(40) Tang, H. W.; Lu, G. H.; Yang, X. N. *IEEE J. Sel. Top. Quantum Electron.* **2010**, *16*, 1725−1731.
(41) Ye, L.; Zhang, S. Q.; Ma, W.; Fan, B. H.; Guo, X.; Huang, Y.; Ade, H.; Hou, J. H. *Adv. Mater.* **2012**, *24*, 6335−6341.
(42) Shin, M.; Kim, H.; Park, J.; Nam, S.; Heo, K.; Ree, M.; Ha, C. S.; Kim, Y. *Adv. Funct. Mater.* **2010**, *20*, 748−754.
(43) Hoppe, H.; Niggemann, M.; Winder, C.; Kraut, J.; Hiesgen, R.; Hinsch, A.; Meissner, D.; Sariciftci, N. S. *Adv. Funct. Mater.* **2004**, *14*, 1005−1011.
(44) Kumar, A.; Hong, Z. R.; Sista, S.; Yang, Y. *Adv. Energy. Mater.* **2011**, *1*, 124−131.
(45) Du, C.; Li, W. W.; Duan, Y.; Li, C. H.; Dong, H. L.; Zhu, J.; Hu, W. P.; Bo, Z. S. *Polym. Chem.* **2013**, *4*, 2773−2782.
(46) Wang, M.; Li, C. H.; Lv, A. F.; Wang, Z. H.; Bo, Z. S. *Macromolecules* **2012**, *45*, 3017−3022.
(47) Jin, E. Q.; Du, C.; Wang, M.; Li, W. W.; Li, C. H.; Wei, H. D.; Bo, Z. S. *Macromolecules* **2012**, *45*, 7843−7854.
(48) Liu, Q.; Wang, M.; Li, C. H.; Jin, E. Q.; Du, C.; Zhou, J. J.; Li, L.; Bo, Z. S. *Macromol. Rapid. Commun.* **2012**, *33*, 2097−2102.
(49) Qin, R. P.; Li, W. W.; Li, C. H.; Du, C.; Veit, C.; Schleiermacher, H. F.; Andersson, M.; Bo, Z. S.; Liu, Z. P.; Inganas, O.; Wuerfel, U.; Zhang, F. L. *J. Am. Chem. Soc.* **2009**, *131*, 14612−14613.
(50) Song, J. S.; Du, C.; Li, C. H.; Bo, Z. S. *J. Polym. Sci., Part A: Polym. Chem.* **2011**, *49*, 4267−4274.
(51) Li, W.; Qin, R.; Zhou, Y.; Andersson, M.; Li, F.; Zhang, C.; Li, B.; Liu, Z.; Bo, Z.; Zhang, F. *Polymer* **2010**, *51*, 3031−3038.
(52) Tong, M.; Cho, S.; Rogers, J. T.; Schmidt, K.; Hsu, B. B. Y.; Moses, D.; Coffin, R. C.; Kramer, E. J.; Bazan, G. C.; Heeger, A. J. *Adv. Funct. Mater.* **2010**, *20*, 3959−3965.
(53) Liu, X. F.; Su, Y. M.; Perez, L. A.; Wen, W.; Toney, M. F.; Heeger, A. J.; Bazan, G. C. *J. Am. Chem. Soc.* **2012**, *134*, 20609−20612.
(54) Intemann, J. J.; Yao, K.; Yip, H. L.; Xu, Y. X.; Li, Y. X.; Liang, P. W.; Ding, F. Z.; Li, X. S.; Jen, A. K.-Y. *Chem. Mater.* **2013**, *25*, 3188−3195.